

FABRICATION OF POLY(ACRYLONITRILE-CO-VINYL ACETATE)-POLY(N-METHYL PYRROLE) COMPOSITE NANOFIBERS

SUAT CETINER, MARIUS OLARIU^{a,*}, A. SEZAI SARAC^b

Kahramanmaras Sutcu Imam University, Department of Textile Engineering, Avsar, Kahramanmaras, Turkey

^aTechnical University 'Gh. Asachi' Iasi, Department of Electrical Measurements and Materials, Bdul D. Mangeron 53-55, Iasi, Romania

^bIstanbul Technical University, Department of Chemistry, Polymer Science and Technology, Maslak, Istanbul, Turkey

Chemical oxidative polymerization of N-Methyl Pyrrole (NMPy) by cerium(IV) on Poly(Acrylonitrile-co-Vinyl Acetate) matrix in N,N-dimethylformamide (DMF) was performed. Electrospinning technique was used for the preparation of P(AN-co-VAc) solutions with uniformly distributed Poly(N-Methyl Pyrrole) (PNMPy) nanoparticles. In the presence of PNMPy, a new absorption band appeared at 1312 cm^{-1} which corresponds to CH in plane vibration peak. The dielectric properties of nanofiber composites were evaluated on the basis of the complex permittivity. The SEM and AFM images of composite nanofibers showed that the PNMPy nanoparticles with the dimensions of 20-40 nm were distributed homogeneously.

(Received December, 14, 2012; April 20, 2013)

Keywords: P(AN-co-VAc), PNMPy, electrospinning, composite nanofiber

1. Introduction

Intrinsically conducting polymers (ICPs), also referred to as organic semiconductors, are π -conjugated polymers, such as polypyrrole (PPy) and polyaniline that can be easily produced by chemical oxidative polymerization in aqueous solutions of monomers. Conducting polymers have received a great attention in recent years due to their wide range of technological applications in several areas such as capacitors, sensors, light emitting diodes, conductive textiles, electrochromic devices, membranes, rechargeable batteries [1-14]. Among the conducting polymers, polypyrrole and its derivatives are especially suitable for commercial applications due to their high electrical conductivity, environmental stability, stability and ease of synthesis. However, applications of conducting polymers have been limited due to their lack of processibility, flexibility and strength. These limitations can be overcome by coating textile substrates with conducting polymers in order to obtain composites, which possess the mechanical properties of textiles whilst retaining the desirable electrical properties of conducting polymers [15-16]. In this regard, conducting polymer composites are a novel class of materials that combine the mechanical properties of the conventional polymers and electrical properties of the conducting polymers, which are very promising for electrical applications [17]. The emerging fields of smart/intelligent textiles have recently attracted new attention for electrically conductive composite textile structures because of exhibiting a wide variety of outstanding properties such as the ability to dissipate static charges, electrical conductivity, dissipation of microwave energy shielding of electromagnetic radiations, etc. The affinity to several kinds of textile structures (i.e., nanofibers, microfibers and fabrics)

* Corresponding author: molariu@ee.tuiasi.ro

doped with conjugated polymers, allows the formation of composite textile structures with improved electrical properties [18].

In this paper, the electrospinning technique was applied to fabricate P(AN-co-VAc)-PNMPy nanofiber composites in a very homogeneously dispersed solution medium. The composite nanofibers were characterized via spectrophotometric, morphological, and dielectric/electrical analysis methods.

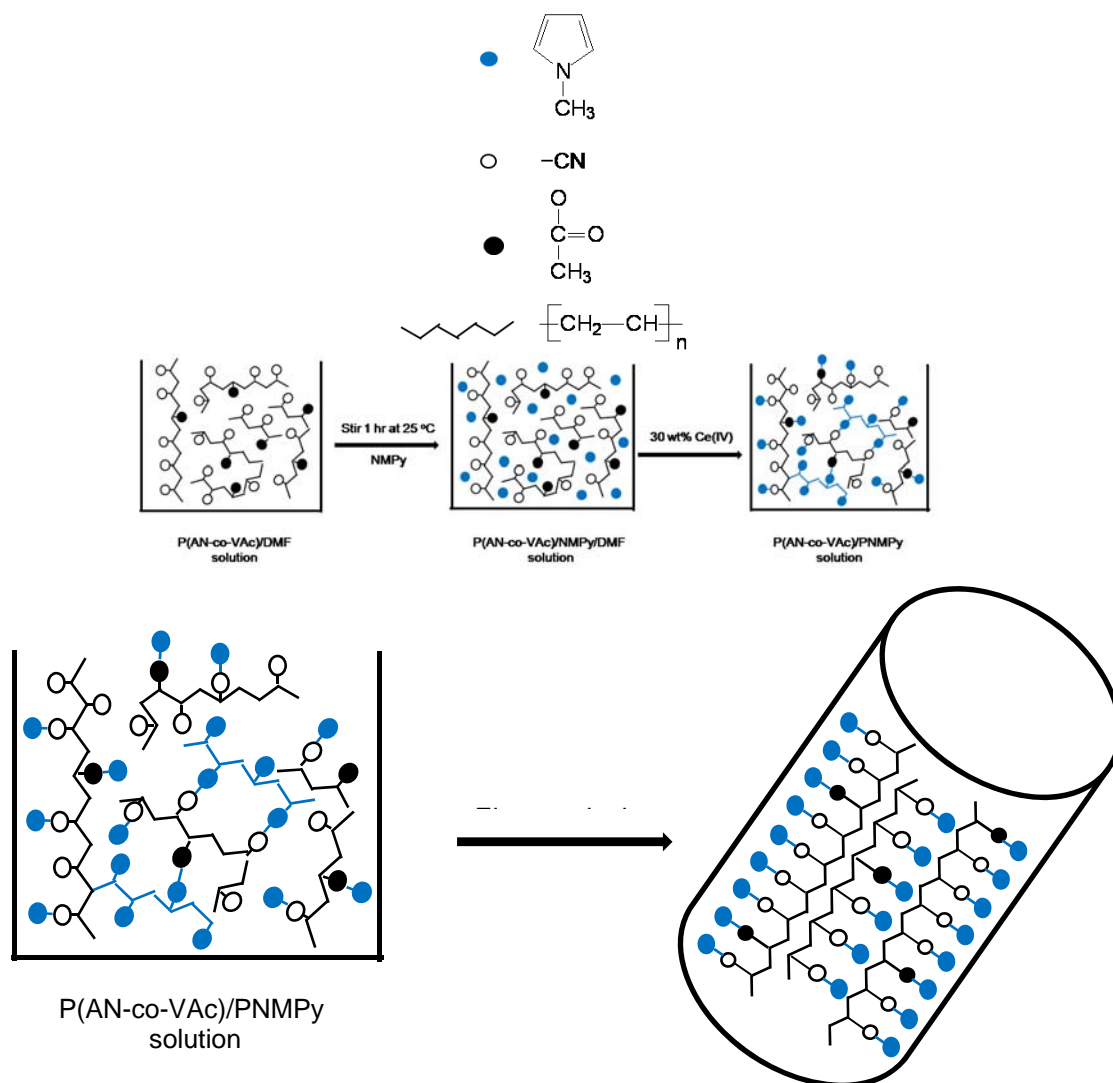


Fig. 1. Schematic illustration of NMPy polymerization on P(AN-co-VAc) matrix and homogeneously distributed PNMPy nanoparticles in composite nanofiber

2. Experimental

2.1 Materials

A PAN copolymer containing 12 wt% vinyl acetate [P(AN-co-VAc)] ($M_w=100.000$) was supplied by Aksa Acrylic (Turkey). Cerium (IV) ammonium nitrate $(NH_4)_2[Ce(NO_3)_6]$ and N,N-dimethylformamide (DMF) were all Merck reagents. N-Methyl pyrrole (NMPy) was supplied by Sigma-Aldrich. All reagents were analytical grade and used without further purification.

2.2. Polymerization of N-Methyl Pyrrole on P(AN-co-VAc) Matrix

P(AN-co-VAc) was dissolved in N,N-dimethylformamide to make a solution with concentration of 10wt% and N-methyl pyrrole with initial mass ratio (10 wt%) was added to above solution. After stirring for one hour at room temperature, Ce(IV) (30 wt% amount of NMPy) was added in order to polymerize NMPy and stirred for about 5 hours 25 °C to obtain PNMPy/P(AN-co-VAc) solution.

2.3. Electrospinning P(AN-co-VAc)-PNMPy Composite Solution

The electrospinning apparatus consisted of a syringe pump (NE-100 model, New Era Pump Systems, Inc., USA), a high-voltage direct current (DC) power supplier generating positive DC voltage up to 50 kV DC power supply (ES50 model, Gamma High Voltage Inc., USA), and a grounded collector that was covered with aluminium foil. The solution was loaded into a 5 mL syringe attached to the syringe pump and was fed into the metal needle. The composite solutions were electrospun at a positive voltage of 17 kV, a working distance of 10 cm (the distance between the needle tip and the collector), and a solution flow rate of 1 mL/h.

2.4 Characterization of Composite Nanofibers

FTIR-ATR spectrophotometric analysis of composite nanofibers was performed by FTIR reflectance spectrophotometer (Perkin Elmer, Spectrum One, with a Universal ATR attachment with a diamond and ZnSe crystal). Morphological studies were performed via scanning electron microscopy (SEM) observations of the composite nanofiber surfaces with a Leo Supra 35 VP scanning electron microscope; and atomic force microscopy (AFM) observations of the nanofiber surfaces with Nanosurf EasyScan2 atomic force microscope. In all AFM analysis, the non-contact mode was employed by using Al coated high resonance frequency silicon tips (190 kHz) with 7 μm thickness, 38 μm mean width, 225 μm length and 48 N/m force constant. The dielectric/electrical measurements were carried out using a Novocontrol Broadband Dielectric Spectrometer (Alpha-A High Performance Frequency Analyzer, frequency domain 0.001 Hz to 3 GHz) at 25 °C. The composite films were placed between two gold-plated electrodes of 20mm diameter.

3. Results and Discussion

3.1. FTIR-ATR Spectrophotometric Analysis

Fig. 2 shows the FTIR spectra of the P(AN-co-VAc)-PNMPy nanofiber composite and pure P(AN-co-VAc) nanofiber.

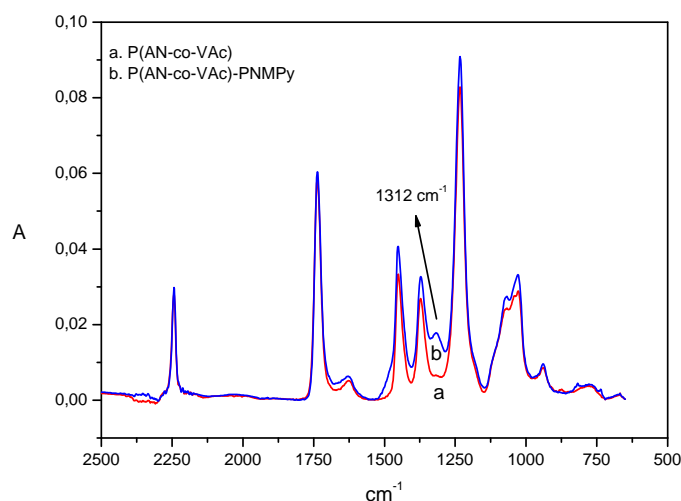
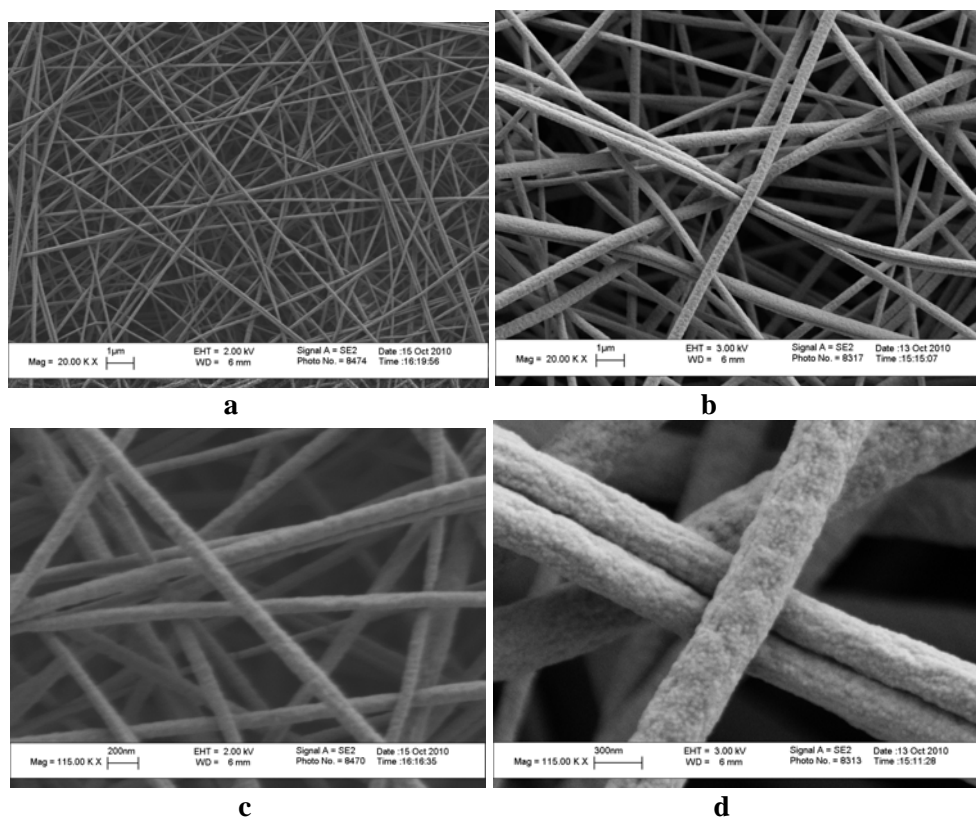


Fig. 2. The FTIR spectra of (a) P(AN-co-VAc) nanofiber and (b) P(AN-co-VAc)-PNMPy composite nanofiber

The absorption bands observed at 2243cm^{-1} , 1453cm^{-1} and 1736cm^{-1} correspond to CN stretching, CH bending and C=O stretching of P(AN-co-VAc), respectively. The other peaks shown at 1229cm^{-1} and 1022cm^{-1} have been assigned for C-O-C stretching and C-O stretching, respectively [19-21]. The band at 1330cm^{-1} corresponds to C-H deformation in chemically synthesized PNMPy [22]. The peak at 1318cm^{-1} is attributed to the ring stretch of PNMPy units [23]. In the presence of PNMPy, a new absorption band appeared at 1312cm^{-1} corresponds to CH in plane vibration peak [Figure 2]. Thus, the FTIR spectrum confirms the polymerization of N-Methyl Pyrrole on P(AN-co-VAc) matrix and incorporation of PNMPy into the nanofiber composite.

3.2. Morphology

Surface morphologies of composite nanofibers were investigated by scanning electron microscope and atomic force microscope in the absence and in the presence of PNMPy. The morphologies of electrospun composite nanofibers are presented in Figures 3(a)–(f).



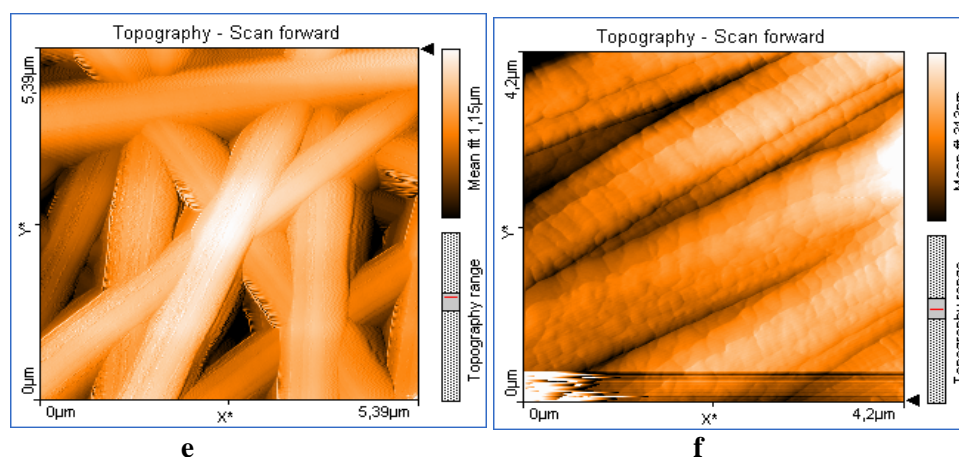


Fig. 3. SEM and AFM images of nanofibers prepared by electrospinning technique ((a),(c)) SEM images of P(AN-co-VAc) nanofibers, ((b),(d)) SEM images of P(AN-co-VAc)-PNMPy composite nanofibers, (e) AFM image of P(AN-co-VAc) nanofiber and (f) AFM image of P(AN-co-VAc)-PNMPy

By comparing Figure 3(a,c,e) and (b,d,f) it is clearly observed that the the surface of P(AN-co-VAc)-PNMPy composite nanofiber is different from P(AN-co-VAc) nanofiber surface. Figures 3 (a,c,e) present that P(AN-co-VAc) nanofibers have more uniform and nonporous smooth morphology. The surfaces of P(AN-co-VAc)-PNMPy composite nanofibers shown in Figure 3(b),(d),(e) exhibit a rough surface structure constructed by uniformly distributed nanosized particles than those of P(AN-co-VAc) nanofibers.

In this regards, the SEM and AFM micrographs of the P(AN-co-VAc)-PNMPy composite nanofibers show the incorporation of homogeneously distributed PNMPy nanoparticles with the dimensions of 20-40 nm in nanofiber composite structure.

3.3. Dielectric/Electrical Behavior

The dielectric properties of nanofiber composites were evaluated on the basis of the complex permittivity, $\epsilon^*(\omega)$. Mathematically it can be represented as a combination of the real part, $\epsilon'(\omega)$, and the imaginary part, $\epsilon''(\omega)$. [24]

$$\epsilon^*(\omega) = \epsilon'(\omega) - i\epsilon''(\omega)$$

The real part is known as dielectric constant, a parameter which is describing the ability of the material to store energy, while the imaginary part is characterizing the capacity of the material of dissipating energy. The analysis of the dielectric parameters versus frequency and/or temperature is providing information in relation to polarization mechanisms when the material is submitted to an electric field.

Below, for analyzing the dielectric properties evolution of P(AN-co-VAc) and P(AN-co-VAc)-PNMPy, parameters as dielectric constant, the dependence of dielectric loss/loss factor and AC conductivity versus frequency is presented [Figure 4].

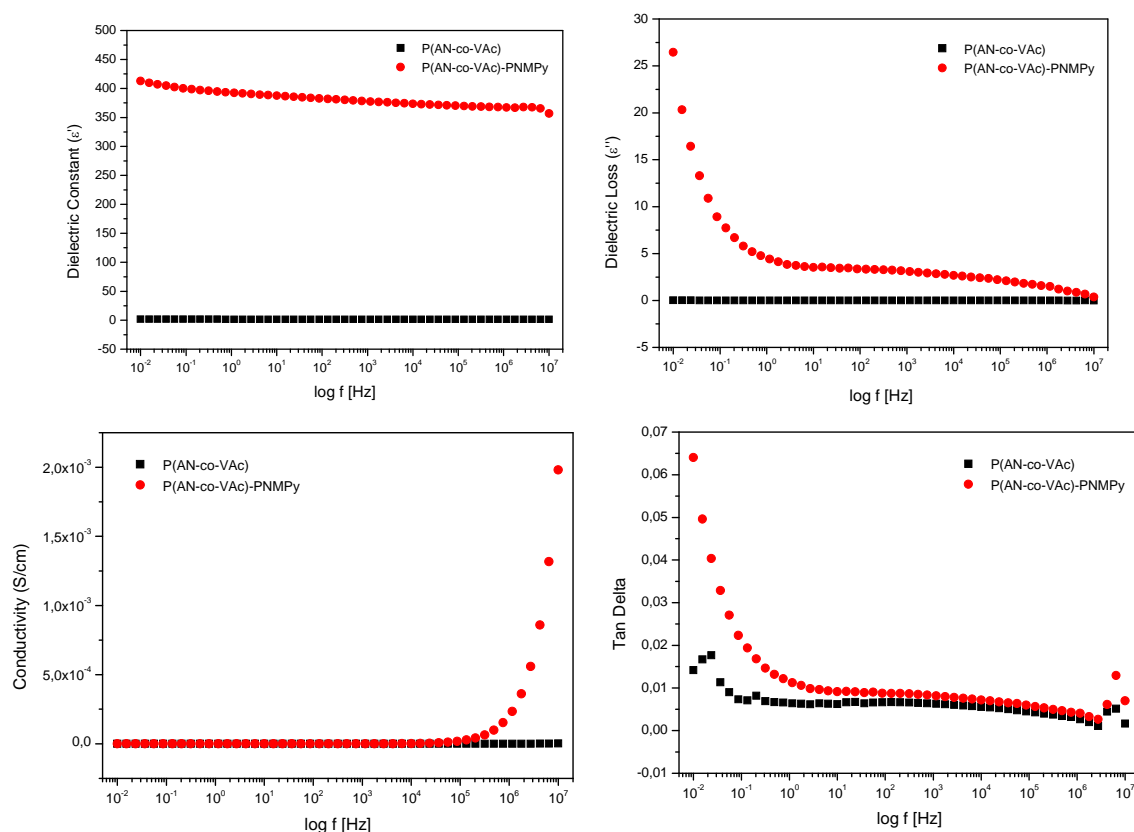


Fig. 4. Dependence of dielectric constant (a), dielectric loss (b), AC conductivity (c) and tan delta (d) of P(AN-co-VAc) and P(AN-co-VAc)-PNMPy composite nanofibers

As it can be observed in Fig. 4, the values of the dielectric parameters measured for the P(AN-co-VAc) matrix, are significantly lower than the ones observed for the P(AN-co-VAc)-PNMPy. In regards to the dielectric constant, a consistent increase of its values can be noticed after oxidative polymerization of N-Methyl Pyrrole (NMPy) by cerium(IV) on Poly(Acrylonitrile-co-Vinyl Acetate) matrix in N,N-dimethylformamide (DMF).

On the other hand, a second relaxation phenomenon can be observed in case of the P(AN-co-VAc)-PNMPy. The relaxation is spreading over a wider domain of frequency but is not very visible and may be due to the dipoles or polar which are rotating in the direction of the applied electric field. Considering the frequencies to which it is occurring, and the relative long time for its occurrence, and the values of dielectric constant over this domain of frequencies, we assume that is about the so-called orientation polarization which can be associated to formation of more polar groups during P(AN-co-VAc)-PNMPy processing. [25]

The high values of loss factor at low frequencies in case of P(AN-co-VAc)-PNMPy are due to Maxwell/Wagner and/or electrode polarization which can be observed when the electric field is applied. Practically, at lower frequencies, the charges have enough time to move towards the interfaces between the P(AN-co-VAc) and P(AN-co-VAc)-PNMPy (Figure 4) or to electrode-polymer interface. [26].

4. Conclusions

A new absorption band observed at 1312cm^{-1} corresponds to CH in plane vibration peak indicating the incorporation of PNMPy in the nanofiber composite. The surfaces of P(AN-co-VAc)-PNMPy composite nanofibers exhibit a rough surface structure constructed by uniformly distributed PNMPy nanoparticles with the dimensions of 20-40 nm in nanofiber composite than those of P(AN-co-VAc) nanofibers. In regards to the dielectric constant, a consistent increase of its values can be noticed after polymerization of NMPy by cerium(IV) on P(AN-co-VAc) matrix. The

high values of loss factor at low frequencies in case of P(AN-co-VAc)-PNMPy are due to Maxwell/Wagner and/or electrode polarization which can be observed when the electric field is applied. The P(AN-co-VAc)-PNMPy nanofiber composites could be preferred for electrically semiconductive material in various fields; such as, electromagnetic shielding, antistatic and capacitor applications.

Acknowledgement

This work was supported by the Scientific and Technological Research Council of Turkey (TUBITAK) and by the project PERFORM-ERA "Postdoctoral Performance for Integration in the European Research Area" (ID-57649), financed by the European Social Fund and the Romanian Government.

References

- [1] Tarkuc S, Sahin E, Toppare L, Colak D, Cianga I., Yagci Y. *Polymer* **47**, 2001 (2006).
- [2] Bittihm R, Ely G, Woelffer F, Munstedt H, Narmann H, Naegele D. *Makromol Chem Makromol Symp* **8**, 51 (1987).
- [3] Mermillod M, Tanguy J, Petiot F. *J Electrochem Soc* **133**, 1073 (1986).
- [4] Hwang LS, Ko JM, Rhee HW, Kim CY. *Synth Met* **55**, 3671 (1993).
- [5] Slater JM, Watt EJ, Freeman J, May JP, Weirm DJ. *Analyst* 1992;117:1265.
- [6] Kudoh Y. In: Aldissi M, editor. *Intrinsically conducting polymers*. London: Kluwer Academic; 1993. p. 191.
- [7] Miller JS. *Adv Mater* **50**, 671 (1993).
- [8] Martin R, Liang W, Menon V, Parthasarathy R, Parthasarathy A. *Synth Met* **55**, 3766 (1993).
- [9] Kraft A, Grimsdale AC, Holmes AB. *Angew Chem, Int Ed* **37**, 403 (1998).
- [10] Burroughes JH, Bradley DDC, Brown AR, Marks RN, Mackay K, Friend RH, et al. *Nature* **347**, 539 (1990).
- [11] Gustafsson JC, Inganas O, Anderson AM. *Synth Met* **62**, 17 (1994).
- [12] DePaoli MA, Panero S, Passerini S, Scrosati B. *Adv Mater* **2**, 480 (1990).
- [13] Sotzing GA, Reynolds JR, Steel P. *J Chem Mater* **8**, 882 (1996).
- [14] Molina J, Del Río, AI, Bonastre J, Cases F. *European Polymer Journal* **44**, 2087 (2008).
- [15] Kaynak A, Beltran R. *Polymer Int* **52**, 1021(2003).
- [16] Cetiner S, Kalaoglu F, Karakas H, Sarac AS. *Fibers and Polymers* **12**, 151 (2011).
- [17] Cetiner S, Kalaoglu F, Karakas H, Sarac AS. *Polymer Composites* **32**, 546 (2011).
- [18] Cucchi I, Boschi A, Arosio C, Bertini F., Freddi G, Catellani M. *Synthetic Metals* **159**, 246 (2009).
- [19] Dong F, Li Z, Huang H, Yang F, Zheng W, Wang C. *Mater. Lett*; **61**, 2556 (2007)
- [20] Sugahara Y, Satokawa S, Kuroda K, Kato C. *Clay. Clay Miner* **38**, 137 (1990).
- [21] Park JY, Lee IH, Bea GN. *J. Ind. Eng.Chem*; **14**, 707 (2008)
- [22] Redondo MI, Sanchez de la Blanca E, Garcia MV, Raso MA. *Synthetic Metals* **122**, 431(2001).
- [23] Duran B, Bereket G. *Ind. Eng. Chem. Res.* **51**, 5246 (2012).
- [24] F Kremer & A Schonhals (Eds), *Broadband Dielectric Spectroscopy*, Springer Verlag 2003;
- [25] *Dielectric Investigation of Doped Poly (methyl acrylate) (PMA) Conducting Polymer Films*, Proceedings of the World Congress on Engineering and Computer Science 2011 Vol II WCECS 2011, October 19-21, 2011, San Francisco, USA.
- [26] F. Kremer, A. Sergej, J. R. Sangoro, M. Treß, and E.U. Mapesa, "Broadband Dielectric Spectroscopy in Nano-(Bio)-Physics"; Proc. ESA Annual Meeting on Electrostatics 2010, Paper F1, pg.1-20;

